Microstructure variation of smoke aerosols in a closed volume

R.F. Rakhimov, V.S. Kozlov, M.V. Panchenko, A.G. Tumakov, and V.P. Shmargunov

Institute of Atmospheric Optics,
Siberian Branch of the Russian Academy of Sciences, Tomsk

Received December 28, 2000

Based on a comparison of the polarization measurement data on aerosol light scattering with the model calculations, the dynamics of microstructure variations of pyrolysis smoke set on in a closed volume is examined. Peculiarities in the transformation of disperse composition of the smoke aerosols on different scales of size spectrum are discussed.

Introduction

Many natural and anthropogenic processes leading to thermal decomposition and sublimation of different materials generate great amount of microdisperse aerosols and aerosol forming compounds into the atmosphere, which actively participate in the formation of the disperse component on the global scale and affect radiative and optical properties and ecological state of the environment. In this paper we analyze optical measurement data obtained using the method of polarization nephelometry to the study of dynamics of microstructure variations of smokes set in a closed volume.

Smoke aerosol was generated resulting from low-temperature thermal decomposition of wood materials, i.e. in the pyrolysis regime. The process of formation of the disperse composition of smoke aerosols was studied in a chamber at the relative humidity of air of 30–40% and temperature of ~ 20°C. The smoke particles filled the aerosol chamber of the nephelometer of the volume of ~ 0.1 m^3. The components of the scattering phase function $g_1(\theta)$ and $g_2(\theta)$ were measured successively in cross polarized light with the wavelength of 0.63 μm in the range of scattering angles $\theta = 5–170°$ by means of a nephelometer. Measurement time needed to acquire a scattering phase function for one polarization was approximately 3 min, the relative error being 5–10%.

Angular dependences of the scattering phase function for unpolarized radiation (directional scattering coefficient) $g(\theta) = (g_1(\theta) + g_2(\theta))/2$ and the degree of linear polarization $p(\theta) = [g_1(\theta) - g_2(\theta)]/[g_1(\theta) + g_2(\theta)]$ were calculated from the recorded data on the polarization components of the scattering phase function.

The diagrams of mutual dynamics of the following parameters of aerosol light scattering were studied in making analysis of the microstructure variations of pyrolysis smokes (using different pair combinations):

– asymmetry coefficients K_a of the scattering phase function $g(\theta)$ equal to the ratio between the light fluxes scattered into the forward and back hemispheres;

– degree of polarization at the angles of $\theta = 110$ and 165° denoted P_{110} and P_{165}, respectively, as well as the ratios $A_s = g(15°)/g(110°)$ and $D_s = g(165°)/g(110°)$, which characterize the degree of peakedness of the scattering phase function in the forward and backward directions.

The diagram approach to analysis of the aerosol scattering parameters has quite a long prehistory.[1–4] The basis for this method was determined by the principle of minimization of the norm of deviation of the selected set of theoretically calculated and experimentally measured parameters of aerosol light scattering. The choice of the above-noted parameters was caused by both numerous experimental and theoretical estimates[1–6] for aerosol formations like atmospheric haze and the content of empirically derived one-parameter model.[7] The parameters A_s and D_s are the ratios of the values of the scattering phase functions which show the maximum dynamics of variations at the change of the atmospheric turbidity, and simultaneously, they have the enhanced sensitivity to variations of the disperse structure and optical constants of the particles of different fractions.

The values of the degree of polarization at the angle $\theta = 110°$ are quite sensitive to the changes in the size spectrum of both microdisperse and accumulative fractions (the mode widths and modal radii of the distributions), as well as to the mutual dynamics of their integral signs of the microstructure. In contrast, the values P_{165} and the asymmetry coefficient of the scattering phase function K_a are sensitive to the size distributions and refractive indices of intermediate and coarse fractions of the hazes, while the parameter D_s is quite sensitive to the model value of the complex refractive index (CRI) of the particulate matter, especially to its imaginary part ("slightly sloping" type of the scattering phase functions for strongly absorbing particles[4]). The values of the refractive index are also important for adequate model estimation of the asymmetry of the scattering phase function. As subsequent model estimates show, the aforementioned parameters of aerosol light scattering selected in such a way in different pair combinations make it possible to follow up quite fine variations in the microstructure of smoke aerosols.

0235-6880/01/08 624-05 $02.00

Results

Regardless of wide dynamics of variations in the conditions of the experiment, it was revealed that the microphysical image of smoke particles shows some stable features of formation, that are caused by the efficiency of smoke formation. It is related to the volume density of smoke in the air (i.e., the maximum reachable level of the particle number density in different size ranges), as well as to the parameters determining the subsequent dynamics of coagulation transformation by means of dry deposition.

Six types of diagrams generalizing practically about 500 experimentally obtained angular dependences of the scattering phase functions and degree of polarization were used for analysis of the observations performed.[4,5] Comparison of the optical characteristics of smokes with the calculated data for some principal types of atmospheric aerosol has shown that the smokes are similar to atmospheric hazes in the peculiarities of the shape and range of variations.

Numerical estimates of the parameters of aerosol light scattering obtained on the basis of three-fraction model of the size spectrum[6,7]

$$n(r) = \frac{dN}{dr} = Ar^{-3} \sum_{i=1}^{3} M_i \exp\{- b_i [\ln(r/r_{mi})]^2\} \quad (1)$$

were used for the diagram analysis of the experimental data.

The hypothesis on independent variations of the CRI values of each fraction was needed in comparing the model data with some measurement results. At the model imitation of the dynamics of variations of the microstructure parameters of the distribution (1), the authors relied on working hypotheses following from the results of direct modeling. For example, the process of coagulation transformations of the disperse structure, which continuously accompanies all other processes determining the formation of smoke aerosol size spectrum, especially in closed volumes, was naturally considered for the fine fraction ($i = 1$) as the main working hypothesis – original cause of the coordinated dynamics of variations in the modal radius and the distribution mode width.

The diagram of mutual variation of the parameters characterizing the degree of backward, D_s, and forward, A_s peakedness of the scattering phase function from the measured results on smoke aerosols (curve *6*) and model estimates (*1–5*) is shown in Fig. 1. The change of the position of points in the diagram along the straight lines (*1–5*) is caused by variations in the disperse structure of aerosol, while the change from one curve to another is caused by variations in the refractive index, which was changed uniformly for all the three fractions in this realization. Thus, it is easy to see from comparing the model data and the results measured at settling the smoke aerosols in a closed volume, that noticeable changes of both disperse composition and the refractive index occur. The diagram shown makes it possible not only to determine the range of variations of the microstructure parameters, but also to obtain the data on the tendencies in variations at different stages of the development of the smoke microstructure.

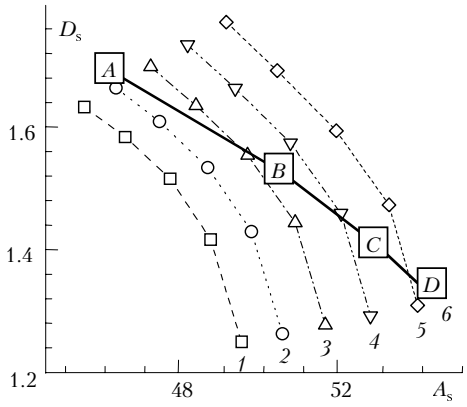

Fig. 1. Diagrams of mutual change of the parameters determining the forward A_s and backward D_s peakedness of the scattering phase function. Calculated data in comparison with experimental ones for $\beta_0 = 0.220$ m^{-1}: $m_1 = 1.595 - i \cdot 0.018$ (□); $m_2 = 1.587 - i \cdot 0.017$ (○); $m_3 = 1.580 - i \cdot 0.016$ (△); $m_4 = 1.572 - i \cdot 0.015$ (▽); $m_5 = 1.565 - i \cdot 0.014$ (◇); *A*, *B*, *C*, *D* – experiment.

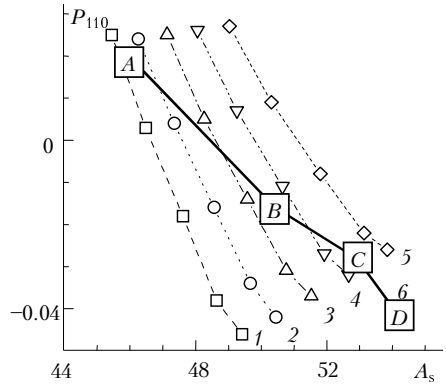

Fig. 2. Diagrams of mutual change of the degree of polarization P_{110} at the angle of 110° and the forward peakedness of the scattering phase function of smoke aerosol A_s. Calculated data in comparison with the experimental ones for $\beta_0 = 0.220$ m^{-1}. Designations are the same as in Fig. 1.

The diagram of mutual change of the degree of polarization of scattered radiation P_{110} and the forward peakedness of the scattering phase function of smoke aerosol A_s (Fig. 2) was considered using the same initial hypotheses on the dynamics of microphysical parameters of smokes. In general, the conclusions on the range of variations of the disperse structure and the refractive index, which follows from Fig. 2, coincide with the conclusions on the analysis of Fig. 1. A little bit poor coincidence between the tendencies of the mutual change of microstructure parameters is acceptable, because they can be caused by instrumental errors in recording the parameters analyzed in the experiment.

The hypotheses on the microstructure variations of smokes introduced are quite realistic as is confirmed by the diagrams of mutual dynamics of the forward A_s (Fig. 3) or backward D_s (Fig. 4) peakedness and K_a of the scattering phase function.

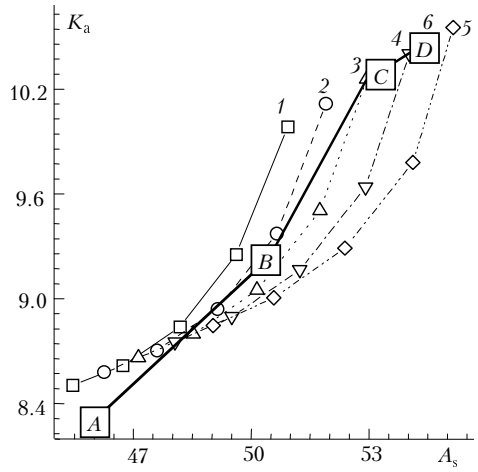

Fig. 3. Diagrams of mutual change of the asymmetry coefficient of the scattering phase function K_a and forward peakedness A_s. Calculated data in comparison with the experimental ones. Designations are the same as in Fig. 1.

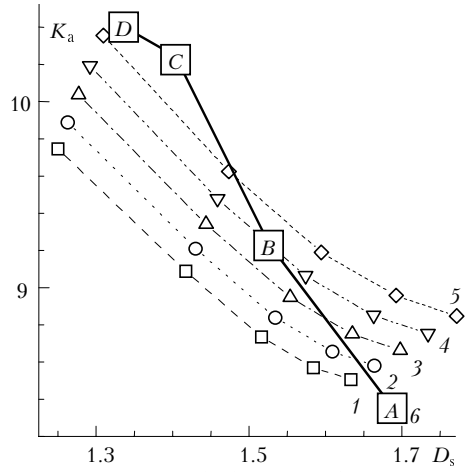

Fig. 4. Diagrams of mutual change of the asymmetry of the scattering phase function K_a and backward peakedness D_s. Calculated data in comparison with experimental ones. Designations are the same as in Fig. 1.

The lack of coincidence between the experimental data and the model ones, seen in Fig. 1 and Fig. 4 is caused, on the one hand, by more complicated technique for determination of the asymmetry of the scattering phase function K_a, incompleteness of the initial data on light scattering in the aureole range and in the range of radar angles $\vartheta = 180°$, and, on the other hand, by spherical idealization of the shape and microstructure of smoke particles in the numerical model. It is well known that light scattering diagram of spherical particles has lower values in the angular range $\theta = 80–110°$ (side scattering) than that of non-spherical particles. Nevertheless, one can see that the results of diagram comparison of the model estimates and measurement data (see Figs. 1–4) provide quite good reasons for qualitative and quantitative conclusions on the microstructure variations of smoke aerosols at their "aging" in a closed volume.

In particular, one can ascertain that the density of smoke at smoke formation is an important scaling factor of formation of optical-microphysical parameters of smoke. The scattering coefficient β_σ increases from 0.006 to 0.3 m^{-1} as the mass of burning material increases from 3 to 20 mg. Polarization measurements show that most stable feature of "aging" the pyrolysis smoke at different smoke densities in a closed volume is the increase of the asymmetry coefficient of the scattering phase function and its forward peakedness at simultaneously decreasing efficiency of light scattering in the backward direction.

When analyzing calculated data, we revealed an ambiguous dynamics in the evolution of the fraction size spectrum, which essentially depends on the mass of the wood sample used for pyrolysis destruction. In particular, the diagram analysis of measurement results shows that transformation of the size spectrum of the fine fraction quite closely follows the coagulation dynamics. The modal radius of particles r_{m1} increases from 0.042 to 0.075 μm. According to the model estimates, the volume merging of coagulating particles occurs at agglutination of particles.

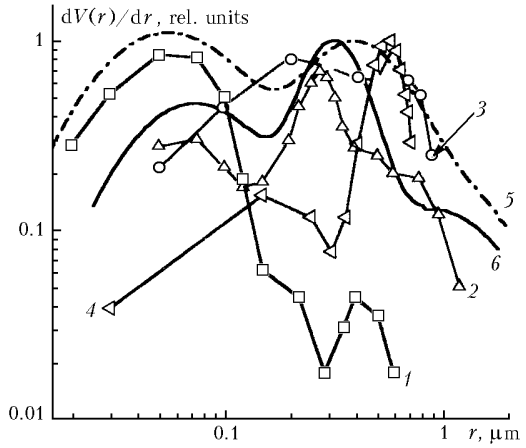

Fig. 5. Size spectrum of smoke aerosols at the beginning (curve *5*) and the end (curve *6*) of the process as compared with the data obtained when solving the inverse problem of light scattering in smokes (curve *3*),[6] (curves *1* and *2*),[9] and the data of Refs. 10 and 11 (curve *4*).

The estimates of the size spectrum dynamics are shown in Fig. 5 as compared with the data obtained when solving the inverse problem of light scattering in smokes,[8,9] as well as with the size spectrum retrieved from measurements of spectral aerosol thickness of the atmosphere. The fact that the revealed dynamics of the change of the size spectrum of dense smokes agrees with the data obtained in Ref. 9 attracts our attention. It was noted in Ref. 12 that the size spectrum of the most coarse smoke particles is displaced to the left on the size scale and becomes narrower, thus forming quite a narrow fraction (see curves *2* and *6*) during the aging at settling of the dense smokes. However, as subsequent model estimates show, the origin of this fraction has a more complicated mechanism of formation.

At the same time, it is important to note that the characteristic size of particles of this fraction is approximately half of the characteristic size of particles of intermediate sizes, which play an important role in the formation of spectral optical thickness of the aerosol component of the atmosphere.[10,11] As subsequent

estimates of coagulation transformation of the size spectrum of fine fraction show, even at anomalously high number density of the fine fraction particles, the process of "coagulation aging," at best, can lead to formation of the selected aerosol fraction with the distribution mode $r_m \cong 0.25–0.30$ μm. In other words, the particles of intermediate sizes revealed at the analysis of mechanism of formation of the anomalous spectral dependence of aerosol optical thickness of the atmosphere result from gravitational selection of aerosol particles at their sedimentation, for example, from stratospheric heights, rather than the "coagulation aging."

To understand the situation on the basis of numerical simulation, let us consider the kinetics of coagulation development of the size spectrum of smoke particles, which was simulated in this paper directly based on the integro-differential Smoluchowski equation complemented with the terms regulating the influence of sink and source of generation of new particles:

$$\frac{\partial n(x,\,t)}{\partial t} = \frac{1}{2}\int_0^x K(x',\,x-x')\,n(x,\,t)\,n(x-x',\,t)\,\mathrm{d}x' - n(x,\,t)\int_0^\infty K(x,\,x')\,n(x',\,t)\,\mathrm{d}x' + \gamma m_j(x,\,t) - \beta n_i(x,\,t), \tag{2}$$

where $K(x, x')$ is the coagulation coefficient of particles of the size x and x', $n(x', t)$ is the particle size spectrum; $n(x)$ is the size spectrum of particles generated by the source; β is the effective rate of particle sink; γ is the rate of generation of new aerosols. Only binary collisions of aerosol particles were taken into account. The dynamics of coagulation development of the fine fraction (with Knudsen numbers Kn lying in the range from 0.05 up to 0.5) was simulated assuming the Brown mechanism of collision with the probability density of collisions

$$K(\nu,\,\tilde{\nu}') = \frac{2kT}{3\mu}\left[\frac{\nu^{1/3}+Al}{\nu^{2/3}} + \frac{\tilde{\nu}^{1/3}+Al}{\tilde{\nu}^{2/3}}\right]\times (\nu^{1/3}+\tilde{\nu}^{1/3})\,n(\nu,\,t)\,n(\tilde{\nu},\,t), \tag{3}$$

where k is the Boltzmann constant, T is absolute temperature, μ is the viscosity of air, A is the Canningham correction, l is the mean free path of molecules, ν and $\tilde{\nu}$ are the volumes of the interacting aerosol particles.

Temporal dynamics of the coagulation change of the size spectra of accumulative and microdisperse fractions of smoke aerosol in submicron size range is shown in Fig. 6 (curves *4–7*).

In particular, it follows from the presented model estimates that the size spectrum of fine particles of pyrolysis origin, which have very high number density, undergoes essential dynamics resulting from coagulation process, and, finally, the fine fraction is transformed to the fraction with the characteristic size in the range 0.17–0.2 μm. It is the fraction that was isolated in Ref. 9 and in this paper from the results of diagram analysis of the data of optical measurements.

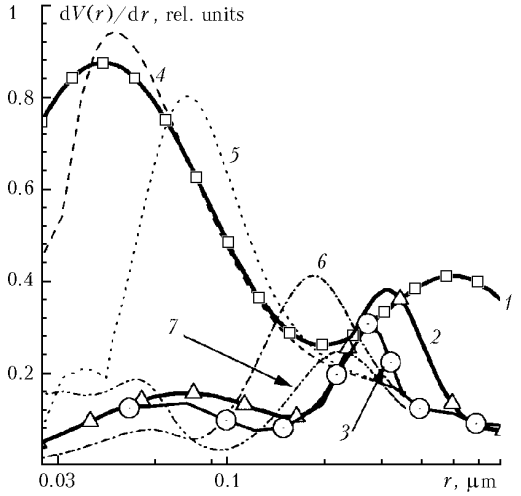

Fig. 6. Dynamics of variations of the size spectrum of smoke aerosols in the process of coagulation with the source of generation and sink to walls (curves *4–7*) as compared with the data obtained by the diagram method (curves *1* and *2*) and solving the inverse problem[9] (curve *3*).

Then, as the process of "coagulation aging" occurred in a closed volume, it was assumed that the source of generation of new particles actively functions during the process. The source power after the stage of pyrolysis essentially decreases, however, generation of new particles continues at subsequent stages of the process from the gas-phase products of thermal sublimation. The lower source power predetermines the lower level of number density of small particles, and, hence, the lower rate of their coagulation development. As a result, the maximum of the volume distribution of particles of the fine fraction of "secondary" (after-pyrolysis) generation during coagulation growth reaches only the size range r_{m1} from 0.042 to 0.075 μm.

At the same time, the dynamics of microstructure parameters of the coarse fraction shows that the most acceptable variant is essential quantitative decrease of both number and volume densities at small displacement of the modal radius r_{m3} from 1.09 to 0.869 μm and relative narrowing of the distribution mode. The last can be related to the active sink of smoke particles to the chamber walls and to the increase of compactness of the morphological structure of the particles of fractal nature.

In this spectral range the process of deposition on the chamber walls prevails over the processes of coagulation increase of the number density of large particles in all considered cases, so the distribution mode gradually gets narrower.

However, it is difficult to explain the peculiarity of the revealed dynamics of the size spectrum of smoke aerosols in the size range 0.4 to 0.8 μm only by the efficiency of the mechanism of dry deposition of smoke particles on the chamber walls. As the particles of this size range are kept in the atmosphere for most long time[4,5,9,10] and undergo the effect of Stokes sedimentation weaker, the revealed dynamics of the size spectrum is rather a consequence of the process of compactification of smoke particles, which were quite

porous at the initial stage of pyrolysis generation and subsequent quick coagulation (at anomalously high number density of monomers). As the diagram dynamics of the light scattering parameters shows, the particles of intermediate sizes coagulate in more dense structures during the smoke change process and become a source of replenishment of the particle fraction with the modal radius of 0.23–0.27 μm, but already to the right of the mode on the size scale.

Thus, the presented results show that the approach we develop in the frameworks of the method of polarization nephelometry is quite a sensitive instrument that provides data for analysis of fine microphysical processes regulating the dynamics of variations of optical and microphysical properties of fine aerosols. In this paper we relied on the measurement data at only one wavelength $\lambda = 0.63$ μm.

In order to essentially expand the potential capabilities of the approach used and to study in more detail the microstructure peculiarities of the mechanism of formation of smoke aerosols and their role in the processes of atmospheric aerosol formation as well as the transformation of their properties under the influence of geophysical factors, it is planned to study these problems in a wider wavelength range on the basis of newly developed flow polarization spectronephelometer.[13]

The spectronephelometer is capable of measuring the scattering phase function $g(\theta)$, the degree of linear polarization $p(\theta)$, and the ellipticity of polarization $q(\theta)$ at five fixed scattering angles $\theta = 15$, 45, 110, 135, and 165°, arbitrarily changing the wavelength in the range $\lambda = 0.4$ to 0.8 μm ($\Delta\lambda \approx 2$ nm). The duration of measurement at one wavelength is 50 s.

The measurement peculiarities are the following. The technique was used for successive measurements of the polarization scattering phase functions (at different states of the beam polarization) and subsequent calculation of $g(\theta)$, $p(\theta)$, and $q(\theta)$; the flow regime of aerosol (the volume of the nephelometer chamber is 5 liters), or collection of one-time samples.

The instrumentation operates in *the regime of automatic measurements* with setting the following parameters: a) wavelengths, b) polarization states of the beam, c) channel numbers, and d) time delay between the cycles of spectral measurements.

The source of radiation is a halogen lamp 100 W/12 V with mechanical modulation of radiation, the frequency is 1 kHz, the beam divergence is 2°, the polarization states of the beam are linear (0, 45, 90, and 135°) and circular.

The receiver of radiation is FEU–84–3 with the field of view of 1° and linear polarization at 45°.

The scattering volume is 5 cm^3, the diameter of the aerosol chamber is 25 cm, and the height is 10 cm.

The sensitivity of the device at measurements of $g(45°, \lambda = 0.52$ μm) is 0.18 $km^{-1}\ sr^{-1}$.

The rms error of measurements is 20%.

Conclusion

Summarizing the results of analysis, let us note that the method of diagram analysis of experimental data obtained by means of polarization nephelometry has the advantage that it makes it possible to outline with certainty the range of microstructure variations of smokes, in which the mutual dynamics of optical parameters (empirical data) forms the consistent unity with a great number of modeled microphysical states. It is more important, because solving the inverse problem is especially difficult, when both the tendencies of the change of not only the size spectrum of smoke aerosols and optical constants of particles are simultaneously unknown.

Diagram comparison of the empirical data with the model estimates makes it possible to obtain such preliminary data which can be useful for solving the inverse problem of light scattering and for a more correct determination of the initial parameters at diagnostics of real microphysical processes that govern the evolution of the state of smoke aerosols under the effect of different factors.

Undoubtedly, subsequent analysis of the parameters of polarization nephelometry taking into account their spectral variability will expand the potential capabilities of the developed approach to investigation of the processes of formation of finely dispersed aerosols.

Acknowledgments

The work was supported in part by Russian Foundation for Basic Research (Grant No. 00–03–32422).

References

1. V.N. Glushko, A.I. Ivanov, G.S. Lifshits and I.A. Fedulin, *Scattering of Infrared Radiation in the Cloudless Atmosphere* (Nauka, Alma-Ata, 1974), 210 pp.

2. G.I. Gorchakov, Izv. Akad. Nauk SSSR, Ser. Fiz. Atmos. Okeana **3**, No. 6, 611–620 (1967).

3. G.I. Gorchakov, A.A. Isakov, and M.A. Sviridenkov, in: *Abstracts of Reports at All-Union Conference on Atmospheric Optics,* Tomsk (1976), Part 1, pp. 230–233.

4. V.S. Kozlov and M.V. Panchenko, Fizika Goreniya i Vzryva **32**, No. 5, 122–133 (1996).

5. R.F. Rakhimov, Atm. Opt. **2**, No. 3, 206–212 (1989).

6. G.M. Krekov and R.F. Rakhimov, *Optical-Radar Model of Continental Aerosol* (Nauka, Novosibirsk, 1982), 200 pp.

7. R.F. Rakhimov and M.V. Panchenko, Atmos. Oceanic Opt. **12**, No. 2, 103–114 (1999).

8. V.V. Veretennikov, I.E. Naats, V.S. Kozlov and V.Ya. Fadeev, Izv. Akad. Nauk SSSR, Ser. Fiz. Atmos. Okeana **16**, No. 3, 270–276 (1980).

9. A.A. Isakov, Atmos. Oceanic Opt. **12**, No. 1, 20–27 (1999).

10. S.M. Sakerin, R.F. Rakhimov, E.V. Makienko, and D.M. Kabanov, Atmos. Oceanic Opt. **13**, No. 9, 754–758 (2000).

11. S.M. Sakerin, R.F. Rakhimov, E.V. Makienko, and D.M. Kabanov, Atmos. Oceanic Opt. **13**, No. 9, 759–765 (2000).

12. R.F. Rakhimov and V.S. Kozlov, Atmos. Oceanic Opt. **11**, No. 9, 792–797 (1998).

13. V.S. Kozlov, M.V. Panchenko, A.G. Tumakov, and V.P. Shmargunov, in: *Abstracts of Reports at VII Workshop on Siberian Aerosols,* Tomsk (2000), p. 113.